



Mechanical properties of sustainable concrete containing powdery ladle furnace slag from different sources

Víctor López-Ausín^a, Víctor Revilla-Cuesta^a, Marta Skaf^{b,*}, Vanesa Ortega-López^a

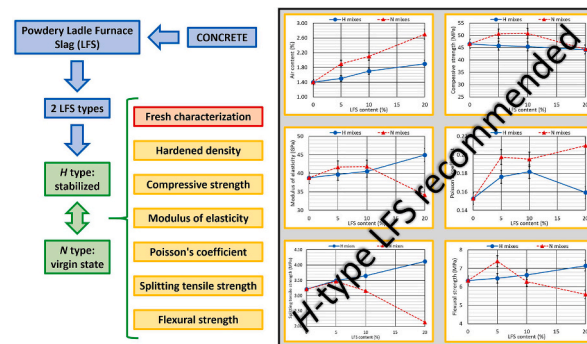
^a Department of Civil Engineering, Escuela Politécnica Superior, University of Burgos, c/ Villadiego s/n, 09001 Burgos, Spain

^b Department of Construction, Escuela Politécnica Superior, University of Burgos, c/ Villadiego s/n, 09001 Burgos, Spain

HIGHLIGHTS

- Concrete produced with Ladle Furnace Slag (LFS) from two different sources.
- *H*-type LFS stabilized before concreting, whereas *N*-type LFS used in original state.
- *H*-type LFS improved all properties except compressive strength, which held constant.
- Up to 10% *N*-type LFS improved compressive behavior, not tensile properties.
- *H*-type LFS recommended, but difference significant only at advanced concrete ages.

GRAPHICAL ABSTRACT



ARTICLE INFO

Keywords:

Concrete
Ladle furnace slag
Pre-treatment
Mechanical performance
Analysis of variance
Multi-criteria optimum mix

ABSTRACT

A suitable content of powdery Ladle Furnace Slag (LFS) has to be selected to balance its hydraulic and expansive properties when added to concrete. In this study, the performance of concrete containing two powdery LFS is studied: *H*-type LFS, stabilized before use, and *N*-type LFS, used in its original state. Lower expansiveness was observed in the *H*-type LFS, and strength development was assisted by the formation of calcium-silicate-hydrates. Therefore, it increased the modulus of elasticity, the splitting tensile strength, and the flexural strength of concrete. Higher hydraulicity and expansiveness were found in the *N*-type LFS, which improved compressive-behavior-related properties up to a content of 10% but reduced tensile-related properties. These aspects were confirmed through scanning electron microscopy. In general, the *H*-type LFS improved the mechanical properties and carbon footprint of concrete, and its use is recommended in a multi-criteria approach, although the difference between both LFS was only statistically significant at advanced ages.

1. Introduction

Concrete production activities, widespread in construction and civil engineering, are undoubtedly essential, due to the large number of

applications in which concrete is used [1,2]. However, its production also has significant environmental impacts, mainly linked to the production of two of its raw materials: aggregate and cement [1,3]. First, aggregates are extracted from quarries and gravel pits, which cause, in

* Corresponding author.

E-mail address: muskaf@ubu.es (M. Skaf).

<https://doi.org/10.1016/j.powtec.2024.119396>

Received 17 November 2023; Received in revised form 19 December 2023; Accepted 7 January 2024

Available online 8 January 2024

0032-5910/© 2024 The Authors. Published by Elsevier B.V. This is an open access article under the CC BY-NC-ND license (<http://creativecommons.org/licenses/by-nc-nd/4.0/>).

addition to a great visual impact on the area [4], the loss of flora and fauna, the emission of large amounts of noise and the alteration of superficial and subterranean water currents and their erosion and sedimentation patterns [5,6]. Besides, CO₂ emissions during cement production are estimated at 0.9–1 tons *per* ton-of-cement produced [7,8]. Pollution levels that make the cement industry one of the highest polluters worldwide [7].

Steel is also among the materials with the widest range of applications. World production of crude steel, accounting for both integral and electric-cycle steelmaking, is currently estimated at two billion tons per year [9]. However, mining of iron ore and siderurgical production also cause significant damage to the environment. Approximately 2.2 tons of CO₂ are emitted into the atmosphere in the production of one ton of steel [10]. Overall, CO₂ emissions from the steelmaking sector currently account for 5% of the world's total emissions of this greenhouse gas [11]. Furthermore, steelmaking activities produce around 250 million tons of slag residues [12], waste with no practical use that has usually been deposited in landfills [13]. However, the search for greater sustainability in both sectors, concrete and steel, has led to convergence. Hence, the current trend to use slag as a raw material in the manufacture of concrete [3,14], not only at the research level, but also in real applications such as building foundations, dams, and submerged concrete components [15–17]. Slag is now processed as a concrete raw material of increasing added value.

A detailed study of the steelmaking industry shows that there are several types of slag [14,18]. One type is blast-furnace slag, produced in blast furnaces in which the smelting of iron ore produces iron, which is alloyed with carbon to produce steel [19]. The stony nature of this type of slag means that it can be used as an aggregate in concrete [20,21], although its cementitious properties also mean that it can be used as a substitute or addition to cement when ground to a powder (ground granulated blast-furnace slag) [22]. Moreover, there is electric-arc-furnace slag, a by-product of electric arc furnaces where scrap steel is smelted for reuse [19]. The high density of this slag makes it a very useful material as an aggregate when concrete needs to reach very high densities [23–25]. Finally, it is necessary, in some cases, to refine the steel from either blast furnaces or electric arc furnaces, to obtain a final commercial product of higher quality [26]. A process that takes place in ladle furnaces [19]. Ladle Furnace Slag (LFS) is obtained during this refining process, and its annual production reaches 30 million tons worldwide [27].

LFS is a powdery white or greyish colored material, although it can be found in large sizes, due to the agglomeration of its particles [26]. Its very variable chemical composition generally contains between 55% and 65% by weight of calcium oxide (lime, CaO) and magnesium oxide (magnesia, MgO); compounds that can be found in both a free and a combined state [28,29]. Silica (SiO₂) and alumina (Al₂O₃) are also generally found in contents between 25% and 35% by weight [28,29]. These compounds form Calcium-Silicate-Hydrates (C-S-H) in the presence of water [13]. However, the expansive properties of both free lime and magnesia in the composition of LFS [30] mean that the hydroxides that form in reaction with water have a larger volume than the initial oxides [31]. Therefore, a recurrent topic in the scarce literature available on the use of LFS in construction materials is the search for a balance between the formation of C-S-H gels that develop strength and the expansiveness of free lime and magnesia [25,32].

The compositions of both LFS and cement are similar [28,29], which means that hydraulic behavior and C-S-H formation may also be observed in LFS [33]. LFS has therefore been introduced into rigid matrices, such as mortars and concretes, generally in substitution of cement [34] or as a cementitious addition [35]. On the one hand, the hydraulic and binder properties of LFS improve the mechanical performance of cement-based materials [36,37]. On the other hand, the addition of LFS in such materials is also risky, since if expansive reactions of the free lime or magnesia occur, the increase in volume when forming hydroxides and carbohydroxides will inevitably result in a

micro-cracking of the matrix of the cement-based material and, therefore, in a worsening of its mechanical behavior [30,38]. Thus, the addition of adequate amounts of LFS in concrete mixes is a key aspect, to find a balance between improved mechanical performance and expansiveness [37]. Nevertheless, LFS can undergo highly variable levels of expansion, such that negligible expansiveness may even be seen in some cases [26,31]. The variability of the expansive performance appears to be linked not only to the chemical composition of the LFS, but also to the stabilization treatment that LFS may undergo before its use, which can cause expansion of the LFS before its addition to concrete [30]. In view of the fact that these aspects are still very scarcely addressed in the literature, it is necessary to define the types and the amounts of LFS that can be added to cement-based materials for effective improvements of their mechanical behavior.

In this study, the mechanical behavior of concrete made with LFS is carefully observed, thus replacing the 0/2 mm aggregate fraction. For this purpose, two factors of the LFS were analyzed in this study: LFS contents varying between 0% and 20%, with the objective of evaluating the effect of LFS content on the mechanical properties, and the source of the LFS, which conditions the stabilization process that it may have undergone prior to its addition to concrete and, therefore, the risk of LFS expansiveness when the LFS is embedded in a rigid concrete matrix [26,30]. The main novelty of this paper is therefore to analyze the effect of the LFS source on the mechanical behavior of concrete, thus defining not only the content but also the source of LFS that yields the best mechanical behavior in concrete. The final objective of this research is to evaluate whether LFS can be used as a value-added raw material in the manufacture of concrete, thus complementing previous research regarding this issue [39,40].

2. Materials and methods

2.1. Raw materials

2.1.1. Conventional raw materials

Following the specifications of EN 197-1 [41], Portland cement CEM II/A-L 42.5 R, with a density of around 3.00 Mg/m³, was used in all the mixes. This cement has a characteristic limestone content of between 6% and 20%, which increases the sustainability of any resulting concrete, and is of standard use in the region where the study was conducted [42].

Two different polycarboxylate admixtures were used: a plasticizer and a viscosity regulator. Their purpose was to assist the concrete to reach the required workability without excessive amounts of water and to retain adequate workability over a longer period of time than it might otherwise. Successful additions of both admixtures are also described in another works of the authors, elsewhere [43].

Two different aggregates were used. First, rounded siliceous aggregate 0/16 mm characterized by an adequate continuous gradation

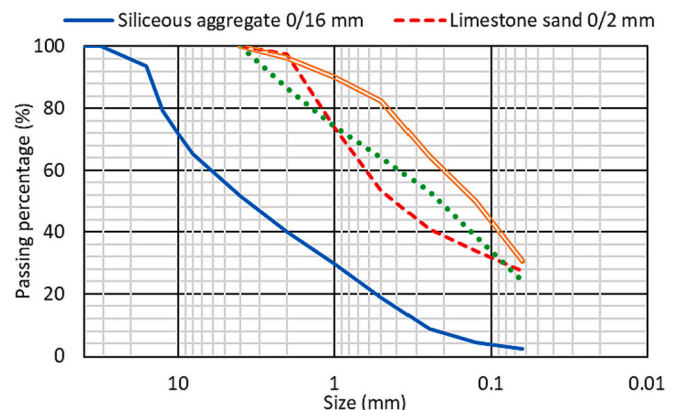


(Fig. 1) that was supplied by a construction materials outlet. The physical properties of both its coarse and the fine aggregate fractions (Table 1) met the standard specifications for concrete manufacturing [44,45]. Besides, limestone sand 0/2 mm was used to complete the granulometry of the siliceous aggregate, providing the fines content necessary for optimum strength development [15]. Its particle size and physical properties (Fig. 1 and Table 1) met the relevant standard specifications [44,45].

2.1.2. Ladle furnace slag (LFS)

Two types of LFS 0/2 mm, labelled type *H* and type *N*, according to the initial letter of the names of the supplying companies, were used to produce the different concrete mixes:

- A suitable amount of the *H*-type LFS was supplied from a waste management company in the steelmaking sector. It had therefore been treated to ensure its stabilization for subsequent disposal at a landfill site. Treatment involved exposure to environmental and meteorological agents, watering, periodic raking and turning, and magnetic removal of any metallic elements. The *H*-type LFS had undoubtedly undergone some hydraulic and expansive chemical reactions during this treatment [31], and, therefore, before concrete production.
- Sufficient *N*-type LFS was obtained directly from a ladle furnace. This LFS had not yet been subjected to any type of treatment for stabilization and landfill disposal, having been poured in a molten state out of the furnace and briefly sprinkled with water for cooling. Therefore, this type of LFS was more unaltered, so it was expected to have a higher chemical reactivity.

The densities of both LFS types showed values of around 2.7 Mg/m³, slightly higher than the density of the limestone sand, as detailed in Table 1. X-ray fluorescence analysis of the chemical composition of the *N*-type LFS presented higher magnesium, iron, and aluminum oxide contents (Table 2), indicative of higher expansiveness (higher content of free magnesia) and higher levels of metallic elements, partly because that slag had not been undergone an aging process. The higher reactivity and unaltered state of the *N*-type LFS also led to higher water absorption of this type of LFS (1.4% vs. 0.4%); to lower levels of particle agglomeration, which resulted in a lower sand equivalent (Table 1) and a gradation with smaller particle sizes (Fig. 1); and to a slightly more irregular shape, as can be noted in the images of each LFS type obtained through Scanning Electron Microscopy (SEM) that are shown in Fig. 2.

Table 1
Physical properties of raw materials.

Property	Standard [41]	Siliceous aggregate 0/16 mm		Limestone sand 0/2 mm	<i>H</i> -type LFS 0/2 mm	<i>N</i> -type LFS 0/2 mm
		4/16 mm	0/4 mm			
Saturated-surface-dry density (Mg/m ³)	EN 1097-6	2.59	2.70	2.66	2.68	2.74
24-h water absorption (%)	EN 1097-6	1.8	0.2	0.1	0.4	1.4
Los Angeles coefficient (%)	EN 1097-2	27	–	–	–	–
Sand equivalent (%)	EN 933-8	–	82	57	41	33

2.2. Mix design

First, the amount of cement, water, and aggregate was defined, based on the specifications of Eurocode 2 [44], for the design of the control mix. Subsequently, as shown in Fig. 3, the proportions of both aggregates, siliceous aggregate 0/16 mm and limestone sand 0/2 mm, were determined by adjusting the overall gradation to the Faury curve, although defining the content of fines <0.063 mm according to the Fuller curve, so as to ensure a concrete of adequate workability and strength. Finally, the water content (water-to-cement ratio of 0.46) and the amounts of the two admixtures (1.9% of cement mass) were adjusted through trial mixes until a slump of 80 ± 20 mm was obtained, which is a standard value specified in EN 206 [41] for a conventional vibrated concrete.

Afterwards, the mixes with LFS were prepared. Concrete mixes were produced in which 5%, 10%, and 20% of the limestone sand 0/2 mm was replaced by each of the two types of LFS 0/2 mm. Thus, it can be said that the LFS was treated as an addition to cement and not as a substitute, so the amount of cement in all the mixes remained constant. The LFS contents were chosen on the basis of experiences from other studies and avoiding the addition of very high percentages, which tended to cause expansion problems in other studies [26,37]. In addition, the water content was adjusted when the LFS was added, thus compensating for its higher water absorption levels, as detailed in Table 1. In this way, the slump remained constant (80 ± 20 mm), and the effective water-to-cement ratio never affected the concrete behavior. The amount of any other component was not modified when LFS was added.

The mixtures were labelled with the letter *V*, in reference to the fact that they were vibrated concrete. Subsequently, a letter, *H* or *N*, was used to indicate the type of LFS incorporated. Finally, a number was entered referring to the added percentage of LFS. The control mix was labelled *V-0* (vibrated concrete with 0% LFS). Table 3 shows the composition of the mixes.

2.3. Mixing process and experimental plan

All the mixes were manufactured using a three-stage mixing process [43], so as to maximize the water absorption of the aggregates and the effectiveness of the admixtures, and thus the workability of concrete. First, the aggregates and half the water were added and mixed for five minutes. Next, the cement, LFS and the remaining water were poured in and mixed for another five minutes. Finally, the admixtures were included, after which the concrete was mixed for another five minutes.

After completion of the mixing process, three fresh-state tests were conducted: slump (EN 12350-2 [41]), fresh density (EN 12350-6 [41]), and air content (EN 12350-7 [41]). Subsequently, different types of specimens were prepared for the mechanical-performance tests, as detailed in Table 4. These specimens were stored in a humid chamber (humidity of 90 ± 5% and temperature of 20 ± 2 °C) until the test age. The mechanical-performance experimental plan was adapted to the volume of concrete that could be produced simultaneously in the laboratory, to ensure adequate comparability of the results by manufacturing all the concrete specimens at the same time. The results of each mechanical test at each age were expressed as the average of the individual test results on three specimens. A micro-structural analysis through JEOL JSM-6460LV scanning electron microscope was also conducted, to support the findings in the mechanical-performance tests. The significance of the effect of the factors on the mechanical behavior was also analyzed through a two-way ANalysis Of VAriance (ANOVA). Finally, the environmental performance of the mixes was evaluated by calculating their carbon footprint, and the optimum mix was determined following a multi-criteria decision-making analysis.

Table 2
Chemical composition of LFS through X-ray fluorescence.

	CaO	SiO ₂	MgO	Fe ₂ O ₃	Al ₂ O ₃	SO ₃	MnO	Others	LOI 110/550 °C *
H-type LFS 0/2 mm	51.67	29.62	6.66	2.79	3.63	1.48	0.42	3.73	3.42/4.71
N-type LFS 0/2 mm	45.58	20.71	15.53	9.67	7.89	2.03	0.31	0.31	0.72/3.95

* Loss of ignition at 110 °C and 550 °C.

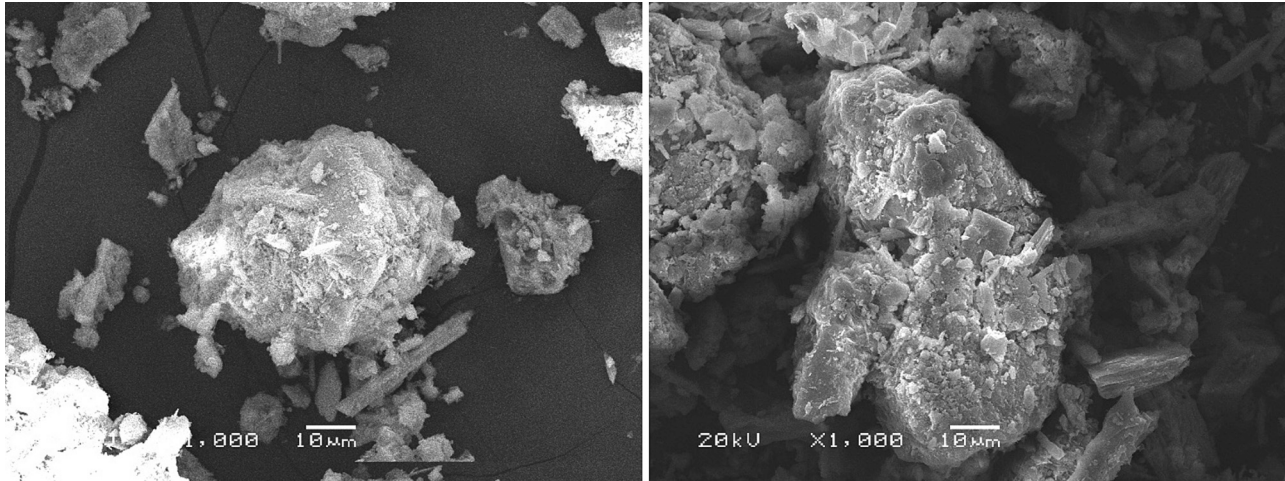


Fig. 2. SEM images of H-type LFS (left) and N-type LFS (right).

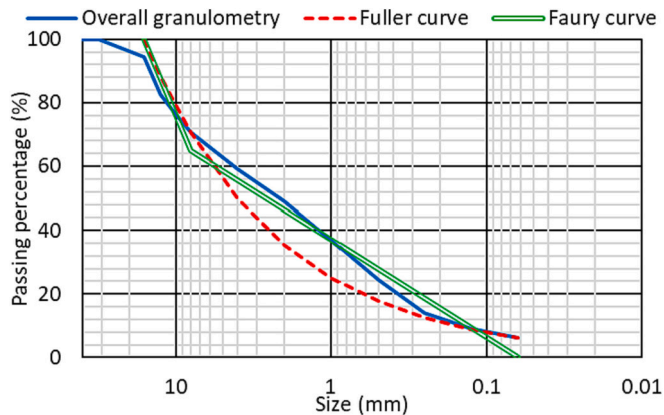


Fig. 3. Overall gradation of the control mix.

Table 3
Mix design (kg/m³).

Component	V-0	V-H-5	V-H-10	V-H-20	V-N-5	V-N-10	V-N-20
Cement	320	320	320	320	320	320	320
Water	149	151	152	156	154	156	162
Plasticizer	4.0	4.0	4.0	4.0	4.0	4.0	4.0
Viscosity regulator	2.0	2.0	2.0	2.0	2.0	2.0	2.0
Siliceous aggregate 0/16 mm	1750	1750	1750	1750	1750	1750	1750
Limestone sand 0/2 mm	320	304	288	256	304	288	256
H-type LFS 0/2 mm	0	16	32	65	0	0	0
N-type LFS 0/2 mm	0	0	0	0	16	32	65

Table 4
Experimental plan of the mechanical-performance tests.

Test	Standard [41]	Age	Specimen type
Hardened density	EN 12390-7	28	10X10X10-cm cubic specimens
Compressive strength	EN 12390-3	7, 28, 90, 180	10 × 20-cm cylindrical specimens
Modulus of elasticity	EN 12390-13	28, 90, 180	10 × 20-cm cylindrical specimens
Poisson's coefficient	EN 12390-13	28, 90, 180	10 × 20-cm cylindrical specimens
Ultrasonic pulse velocity	EN 12504-4	7, 28, 90, 180	10 × 10 × 10-cm cubic specimens
Splitting tensile strength	EN 12390-6	28	10 × 20-cm cylindrical specimens
Flexural strength	EN 12390-5	28, 90	7.5 × 7.5 × 27.5-cm prismatic specimens

3. Results and discussion: Experimental tests

3.1. Fresh behavior

The results of the tests in the fresh state are shown in Fig. 4. Neither of the two types of LFS caused a major change in the fresh behavior of concrete, as the variations were small. However, some trends were discernible:

- The addition of low LFS contents ($\leq 10\%$) led to a general decrease in the slump of the concrete (Fig. 4a), possibly due to the more irregular shape of LFS than limestone sand, which would have increased the internal friction between the concrete components [46]. Moreover, the higher water absorption of the LFS also contributed to the decrease in workability [19]. However, when incorporating higher LFS contents (20%), since the water content had to be adjusted, this modification offset the previous aspects, and increased the final slump (95 mm in the V-H-20 mix). This slump increase may result from incomplete water consumption by higher amounts of LFS,

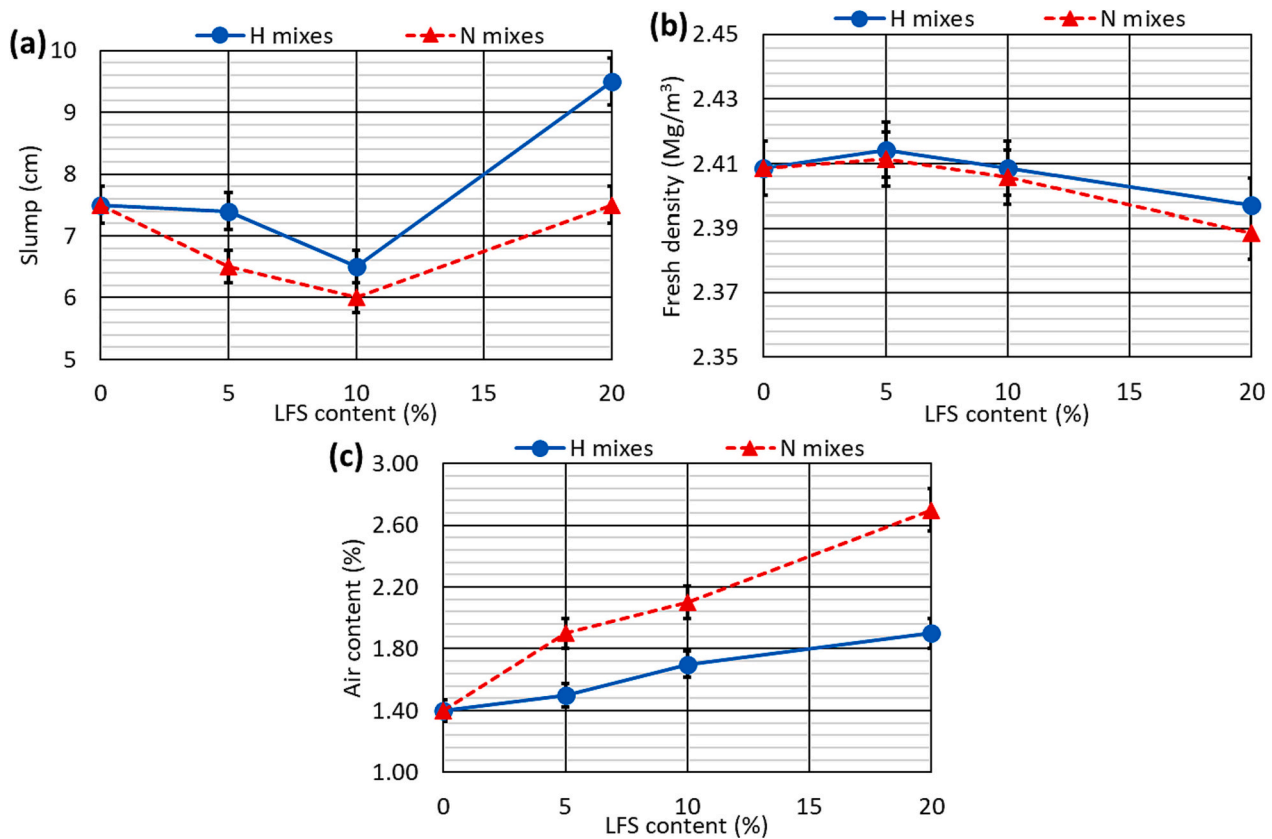


Fig. 4. Fresh tests: (a) slump; (b) fresh density; (c) air content.

which in turn would have increased the workability of concrete [28,36].

- There was no increase in the fresh density of the concrete (Fig. 4b) following the addition of LFS, despite its higher density compared to limestone sand (Table 1), and it even slightly decreased as the content of this waste increased. The increase in water content with the addition of LFS may explain this behavior.
- The air content (Fig. 4c) rose approximately linearly with the LFS content, from 1.40% in the control mix to 1.90% with 20% *H*-type LFS, and 2.70% with 20% *N*-type LFS. Nevertheless, it should be noted that the air-content increases were consistently minimal, below 0.8% in absolute value in almost all the cases, so its effect on the mechanical behavior of the concrete is considered to have been minimal as well.

Analyzing each type of LFS, *N*-type LFS had the most unfavorable effect in the fresh performance of the concrete. Thus, the slump of the concrete with *N*-type LFS decreased by between 10% and 30% compared to the *H*-type LFS. In fact, the *V-N-10* mix had a slump of exactly 60 mm, the minimum value according to the mix design. Likewise, the difference between the air content of the mixes made with the *N*-type LFS was always between 0.50% and 0.80% higher, in absolute terms, than the mixes with the *H*-type LFS. The less altered state of the *N*-type LFS, that resulted in more irregular shapes and higher hydraulic activity, worsened its fresh behavior. However, it should be noted that the worsening of these properties with the addition of LFS was slight and was much better might have otherwise been obtained with other sustainable additions and aggregates [47,48].

3.2. Hardened density

The hardened density of concrete is lower than its fresh density, due to the evaporation of part of the water during the setting process [48].

Thus, the density of the concrete mixes decreased between 2% and 5% from the fresh to the hardened state, as shown in Fig. 5. There was no clear trend in the decrease in density in relation to the LFS content, although the largest decrease occurred in the *V-0* control mix, possibly because the LFS absorbed water during the hydraulic reactions, thus decreasing evaporation [49].

Several aspects can be noted when considering the hardened density. Firstly, evaporation reduced the influence of water on concrete density, so much so that all the mixes with LFS showed a higher density than the control mix, unlike their fresh density. A result that can be explained by the higher density of both types of LFS compared to the limestone sand that they replaced (Table 1). Secondly, the increased content of LFS led to an increase in the water-to-cement ratio of the concrete, which perhaps slightly augmented concrete porosity [43], and to a higher increase in concrete volume as a consequence of the potential expansion of

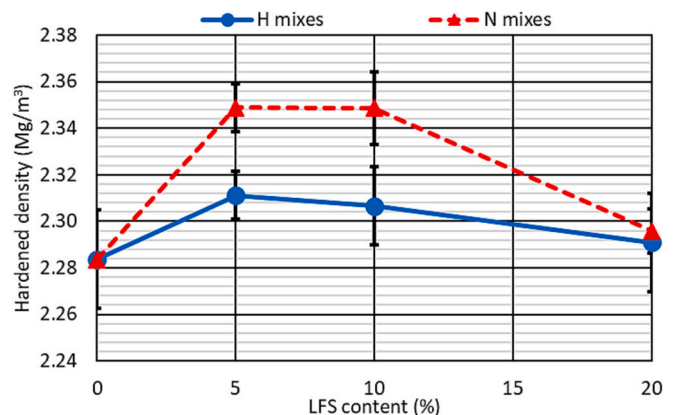


Fig. 5. 28-day hardened density.

the LFS [26]. Both aspects resulted in the hardened density decreasing as the LFS content increased, so that the addition of 20% of both types of LFS led to a hardened density very similar to that of the control concrete (2.29 Mg/m³). Finally, it can be pointed out that the *N*-type LFS produced the greatest increase in the hardened density of the concrete when added at low percentages (density of around 2.35 Mg/m³ for the *V-N-5* and *V-N-10* mixes and of around 2.31 Mg/m³ for the *V-H-5* and *V-H-10* mixes), possibly due to its higher density (Table 1) and hydraulic behavior [19], but it also produced the sharpest decrease in density when added at 20%, due to its more expansive nature [50].

3.3. Compressive strength

The compressive strength of the mixtures was measured at 7, 28, 90, and 180 days, results that are also presented in part and in less depth in another paper for statistical analyses [40]. Both the effect of the LFS at 7 days (early age) and at 180 days (late age), as well as its strength development over time are shown in Fig. 6. After 180 days, all the mixes showed a compressive strength higher than 40 MPa, making them suitable for use in components designed to withstand high stress levels [44,45].

The 7-day and 180-day compressive strengths are shown in Fig. 6a and Fig. 6b, respectively. Each type of LFS led to different compressive-strength evolution trends with the LFS content, although the strength variations when *N*-type LFS was added were greater, presumably due to its higher chemical reactivity [26,36]:

- Additions of 5% and 10% of the *N*-type LFS increased the compressive strength by 5 MPa with respect to the *V-0* mix at both ages. The C-S-H forming reactions that occurred in LFS [13] were the most

relevant for those LFS contents, compensating potential expansive phenomena, so LFS therefore increased compressive strength. 20% *N*-type LFS reduced the strength by 5 MPa at 7 days and 2 MPa at 180 days compared to the control mix. As previously mentioned, LFS contains expansive free lime and free magnesia, which can cause micro-cracking of the concrete matrix and worsen the mechanical behavior of concrete [50,51], effect that was found when this LFS type was added in high amounts. This decrease was lower at 180 days, as it appeared that the formation of C-S-H gel compensated concrete micro-cracking due to expansive reactions more effectively at advanced ages than at younger ages. In addition, the higher strength of the concrete matrix at advanced ages may have also decreased the likelihood of micro-cracking [52], so that the LFS contributed more effectively to strength development.

- All the *H*-type LFS mixes showed very similar compressive strengths to the control mix at both 7 days (35–37 MPa) and 180 days (44–46 MPa). This type of LFS increased or decreased the compressive strength by only 2 MPa, minimum variations as per the results available in the literature [36,37]. As compressive strength increased at 7 days, the micro-cracking of the concrete matrix caused by the *H*-type LFS could be low at early ages, due to its aging prior to concrete production, which in turn could result in the strength-development reactions being the most important. The compressive strength of the concrete with *H*-type LFS was slightly reduced at 180 days, perhaps due to the relevance of the expansive reactions that were higher at advanced ages. Nevertheless, the compressive strength fluctuations were higher for the *N*-type LFS at both ages, possibly due to both its composition and its higher reactivity caused by its untreated state when incorporated in the concrete [30].

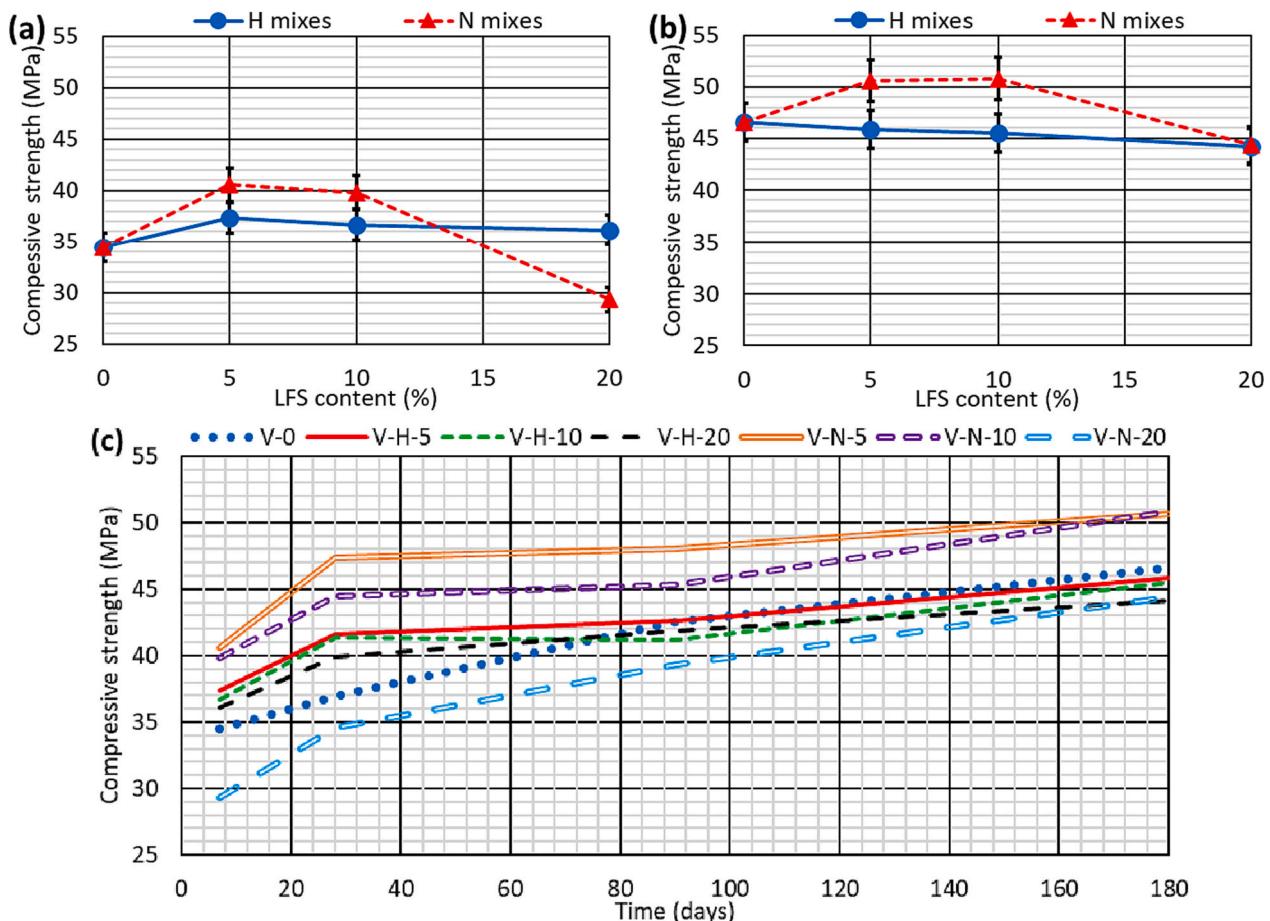


Fig. 6. Compressive strength: (a) 7-day results; (b) 180-day results; (c) development over time.

An analysis of the time evolution of the compressive strength (Fig. 6c) shows that the mixes with 5% and 10% LFS experienced an increase in compressive strength from 7 to 28 days, mainly due to the formation of C-S-H as a consequence of the hydration of the cement and the LFS [13]. Thereafter, the compressive strength remained constant up to 90 days, possibly due to expansive reactions in the LFS that caused micro-cracking in the concrete, which counteracted the effect of hydration [36]. After 90 days, the compressive strength increased again, which was likely due to the fact that the expansive reactions never affected the concrete matrix so noticeably at those ages, because of its higher strength, producing a less important micro-cracking than the formation of C-S-H gel [52]. This behavior was supported by the results found in literature [26,53], which has generally shown that cement-based materials containing LFS are likely to develop higher strength in the long term. In contrast, the compressive strengths of the mixes with 20% LFS exhibited a continuous development of compressive strength. It is thought that the increase in the LFS content led to expansive reactions mainly affecting concrete strength at early ages. The micro-cracking caused by LFS expansion was therefore effectively offset by the hydration reactions at later ages [52]. In this temporal evolution, it was found that the *N*-type LFS led to the most notable increase in strength at advanced ages. Its higher chemical reactivity compared to the *H*-type LFS, caused by its composition and less weathering before its use in the concrete, could have caused the longer-lasting chemical reactions over time [11]. All these discussed aspects resulted in the *V-H-20* and *V-N-20* mixes exhibiting almost the same compressive strength at 180 days.

3.4. Modulus of elasticity

The values of the modulus of elasticity at 28, 90, and 180 days are

depicted in Fig. 7, which are also briefly discussed in another paper as a basis for conducting statistical analyses [40]. The *N*-type LFS had very similar effects on both the modulus of elasticity and compressive strength, while the effects of the *H*-type LFS were on the contrary very different (Fig. 7a and Fig. 7b).

- The *N*-type LFS led to an increase in the elastic stiffness of the mixes when added in amounts of 5% and 10%. An increase that was consistently 3–4 GPa higher with respect to the *V-0* mix, regardless of age. Nevertheless, the modulus of elasticity in the mixes with 20% *N*-type LFS decreased by around 2.5 GPa and 5 GPa at 28 and 180 days, respectively, compared to the control concrete. The formation of C-S-H gels with low additions of LFS was greater than the micro-cracking of the concrete matrix, because of the formation of calcium and magnesium hydroxides [29,38], whence the improved modulus of elasticity of the concrete. However, that micro-cracking was the most relevant phenomenon for high LFS contents. Furthermore, the aforementioned expansion at advanced ages affected the modulus of elasticity, unlike compressive strength; perhaps because of the significant effect of micro-cracking within the interfacial transition zones, which assisted sliding between both aggregate and matrix [52], a key aspect in the elastic modulus of concrete [54].
- The reduced expansion of the *H*-type LFS had no effect on the modulus of elasticity of the concrete. Instead, it was enhanced at all ages when adding this LFS type, due to the chemical reactions of C-S-H gel formation [34]. Amounts of 5% and 10% *H*-type LFS increased the modulus of elasticity in similar ways at both 28 and 180 days (around 2–3 GPa), but an amount of 20% *H*-type LFS increased it much more at 180 days (increases over the *V-H-10* mix of 2 GPa at 28 days and 4.5 GPa at 180 days). Results that showed the high capacity

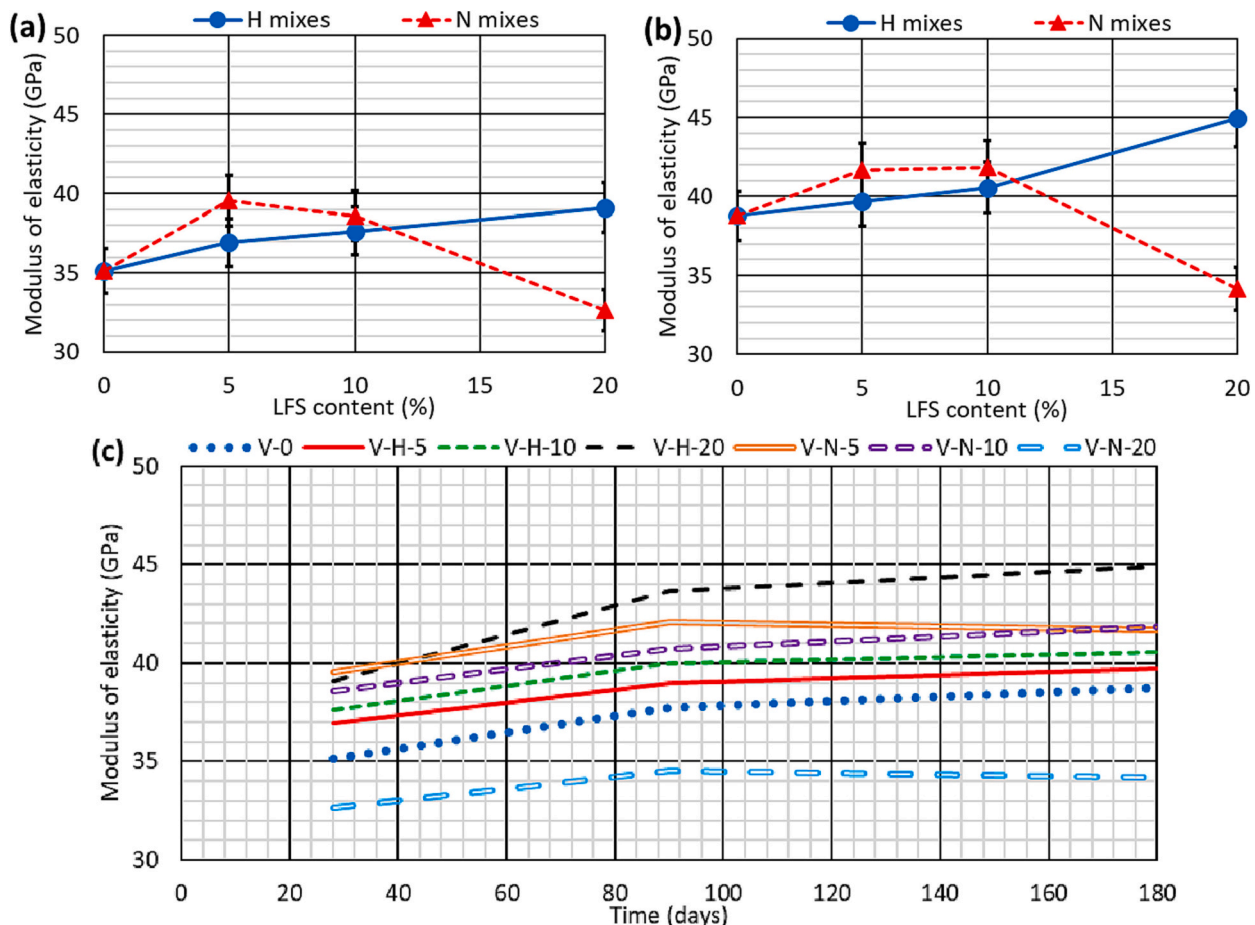


Fig. 7. Modulus of elasticity: (a) 28-day results; (b) 180-day results; (c) development over time.

of the *H*-type LFS to provide elastic stiffness to concrete at advanced ages and that fit with other results in the literature, confirming the capacity of LFS to improve long-term mechanical behavior [49,55].

A comparison of both LFS types revealed that the moduli of elasticity of the mixes with the *N*-type LFS were between 1 GPa and 2 GPa higher for the 5% and 10% LFS contents at all ages. On the contrary, the modulus of elasticity of the *V-N-20* mix was 6.5 GPa lower than that of the *V-H-20* mix at 28 days and 11 GPa lower at 180 days. It is clear that, for both C-S-H gel formation and expansive reactions, the *N*-type LFS showed higher activity, perhaps because of its more unaltered state [52]. This effect was more noticeable for the modulus of elasticity than for the compressive strength, especially at advanced ages.

The evolution of the modulus of elasticity from 28 to 180 days is shown in Fig. 7c. Unlike for compressive strength, there was no clear trend as a function of the percentage of added LFS. Thus, all the mixtures, including the control concrete, showed the highest increases of their moduli of elasticity between 28 and 90 days (90-day modulus of elasticity between 96 and 98% of the 180-day modulus of elasticity), remaining practically constant for later ages. Thus, the addition of LFS meant that this mechanical property followed a similar temporal development to concrete made with Portland cement, as shown for other slag types when used as binders [22].

3.5. Poisson's coefficient

Poisson's coefficient can be defined as the ratio between the transverse strain and the longitudinal strain of a material in an elastic regime [56]. Thus, at the same time as the longitudinal strain was evaluated for determining the modulus of elasticity, the transverse strain was also

measured. So, the Poisson's coefficient at 28, 90, and 180 days could be obtained for all the mixtures, as shown in Fig. 8.

Minimal levels of transverse strain are common in conventional concrete, so an increase in the modulus of elasticity (decrease in longitudinal strain) usually causes a decrease in Poisson's coefficient [44,45]. However, no such behavior was observed in the mixes under study. As shown in Fig. 7, the modulus of elasticity increased with any amounts of *H*-type LFS and with 5% and 10% of *N*-type LFS. However, Poisson's coefficient increased with raising amounts of both types of LFS (Fig. 8a and Fig. 8b). It appears that micro-cracking, due to LFS expansion, increased concrete deformability in the transversal direction to the load direction [35], which compensated for the reduction in longitudinal deformability. Mix *V-H-20* was the only mix to follow the conventional trend, undergoing a high increase in the modulus of elasticity and, as a result, a decrease in the Poisson's coefficient with respect to the mixes with lower contents of the *H*-type LFS.

Analyzing the effect of each type of LFS, the smallest Poisson's coefficients were observed with the *H*-type LFS. So, the difference between the Poisson's coefficients of the *H*-type and the *N*-type LFS mixes when added at amounts of 5% and 10% was around 0.02 units at 180 days (Fig. 8b), although the mixes with *N*-type LFS were observed to have higher elastic moduli. A much lower Poisson's coefficient was observed in the *V-H-20* mix than in the *V-N-20* mix (0.178 vs. 0.202 at 28 days, and 0.159 vs. 0.210 at 180 days). This better performance of the *H*-type LFS can be explained by its lower expansivity, which resulted in transverse deformability increasing less [31] and in longitudinal stiffness increasing more than in the *N*-type LFS mixes [56]. Furthermore, it appeared that the transverse deformability increased in the *N*-type LFS concrete mixes over time, which meant that the behavior of Poisson's coefficient in the *H*-type LFS concrete specimens was better than in the

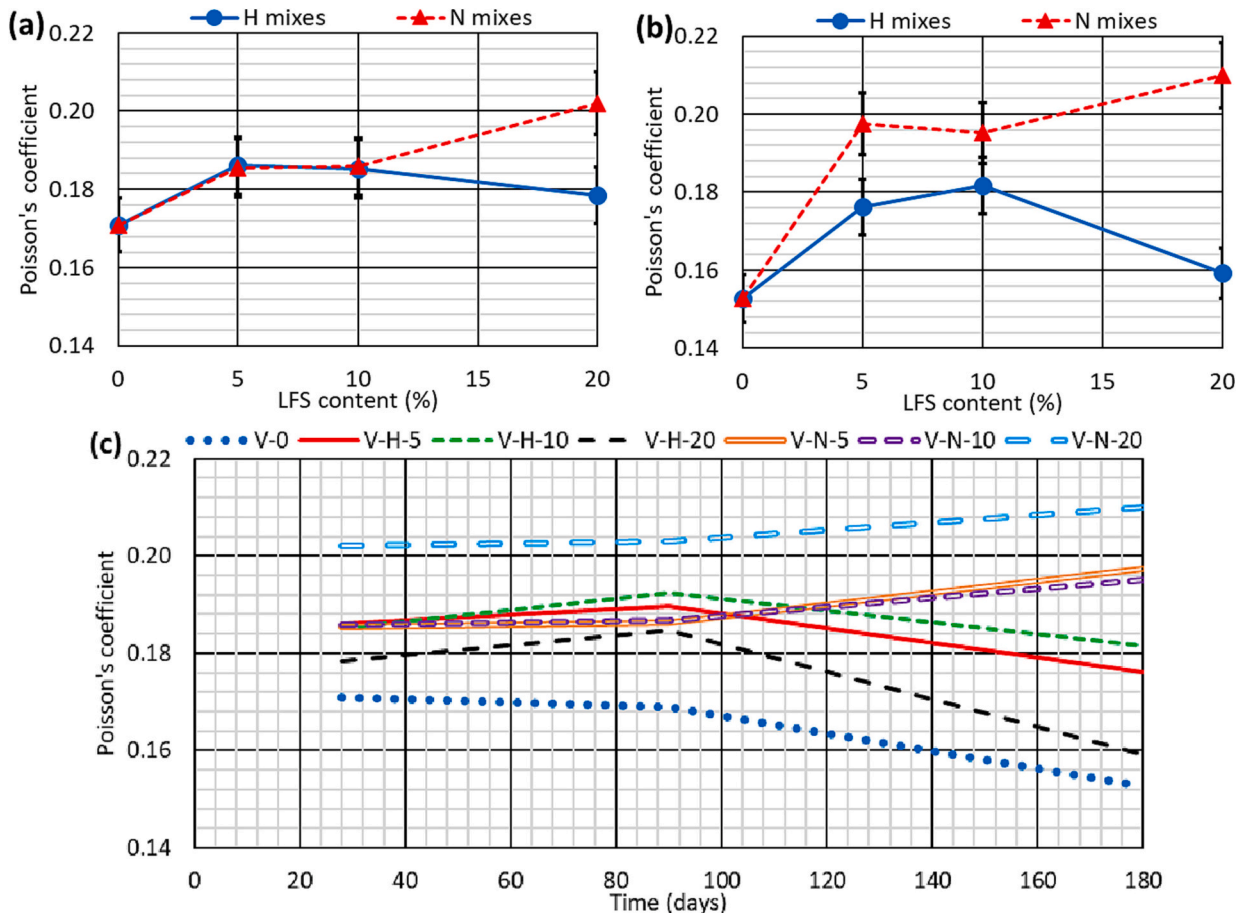


Fig. 8. Poisson's coefficient: (a) 28-day results; (b) 180-day results; (c) development over time.

mixes with *N*-type LFS at advanced ages.

The temporal evolution of Poisson's coefficient is shown in Fig. 8c. The *H*-type LFS mixtures showed an almost conventional temporal evolution of Poisson's coefficient, since a decrease in the value of this ratio was found from 90 days onwards. However, the *N*-type LFS mixtures most clearly exemplified the increase in transverse deformability as a consequence of LFS expansion, a notable increase in Poisson's ratio being observed from 90 to 180 days.

3.6. Ultrasonic pulse velocity (UPV)

Ultrasonic Pulse Velocity (UPV) was determined at 7, 28, 90 and 180 days, as shown in Fig. 9. Generally, this non-destructive measure of concrete quality is related to density, compressive strength, and the modulus of elasticity [57], so UPV can be used for their estimation [58]. In this case, the variation in UPV between the different mixes was minimal (differences between 0.05 km/s and 0.10 km/s). However, the differences in both the compressive strength and, especially, the modulus of elasticity, were appreciable, as detailed in previous sections, so that the UPV would not be an adequate indicator for their estimation. It can be explained by the high variability associated with this non-destructive measurement [57] and because neither the micro-cracking that the concrete matrix may have undergone as a consequence of LFS expansion, nor the additional generation of C-S-H gels notably affected the value of the UPV [26]. Therefore, it is possible that the UPV readings were more conditioned by the concrete density, after adding the LFS, which also presented minimal variations (Fig. 5).

The increase in the content of both types of LFS led to a decrease in the UPV with respect to the value of the *V-0* control mix (4.67 km/s at 7

days and 4.83 km/s at 28 days) at all ages (Fig. 9a and Fig. 9b), although slightly higher values were obtained with the addition of 5%, possibly because of the way LFS affects concrete strength and stiffness [13]. Similarly, the addition of the *N*-type LFS resulted in a decrease of the UPV of around 0.03 km/s compared to the *H*-type LFS mixtures (Fig. 9a and Fig. 9b) for all LFS amounts. Both aspects can be fundamentally linked both to higher micro-cracking caused by the increased LFS content and to the higher reactivity of the *N*-type LFS [31], although both aspects only caused minor UPV variations. Furthermore, it is important to note that 5% and 10% *N*-type LFS led to higher compressive strengths and moduli of elasticity, but to lower UPV readings. An aspect that once again underlines the absence of a strong correlation between these properties for LFS mixtures of this type.

Finally, the temporal evolution of this property (Fig. 9c) shows that the UPV readings of all the mixes increased continuously, albeit minimally, over time. The increase in the UPV readings over time can be attributed to the increase in the stiffness of the cementitious matrix of the concrete, an aspect that explained this same UPV behavior when other alternative binders were used [58,59]. Quite unlike the trend for compressive strength (Fig. 6c) which, for example, remained constant between 28 and 90 days for various mixtures. Results that confirmed the extent to which UPV is not a suitable property with which to estimate how LFS alters the mechanical behavior of concrete.

3.7. Splitting tensile strength

The results of the 28-day splitting tensile strength are detailed in Fig. 10, which along with the flexural strength test results enabled the evaluation of the effect of the LFS under tensile stresses [43]. The

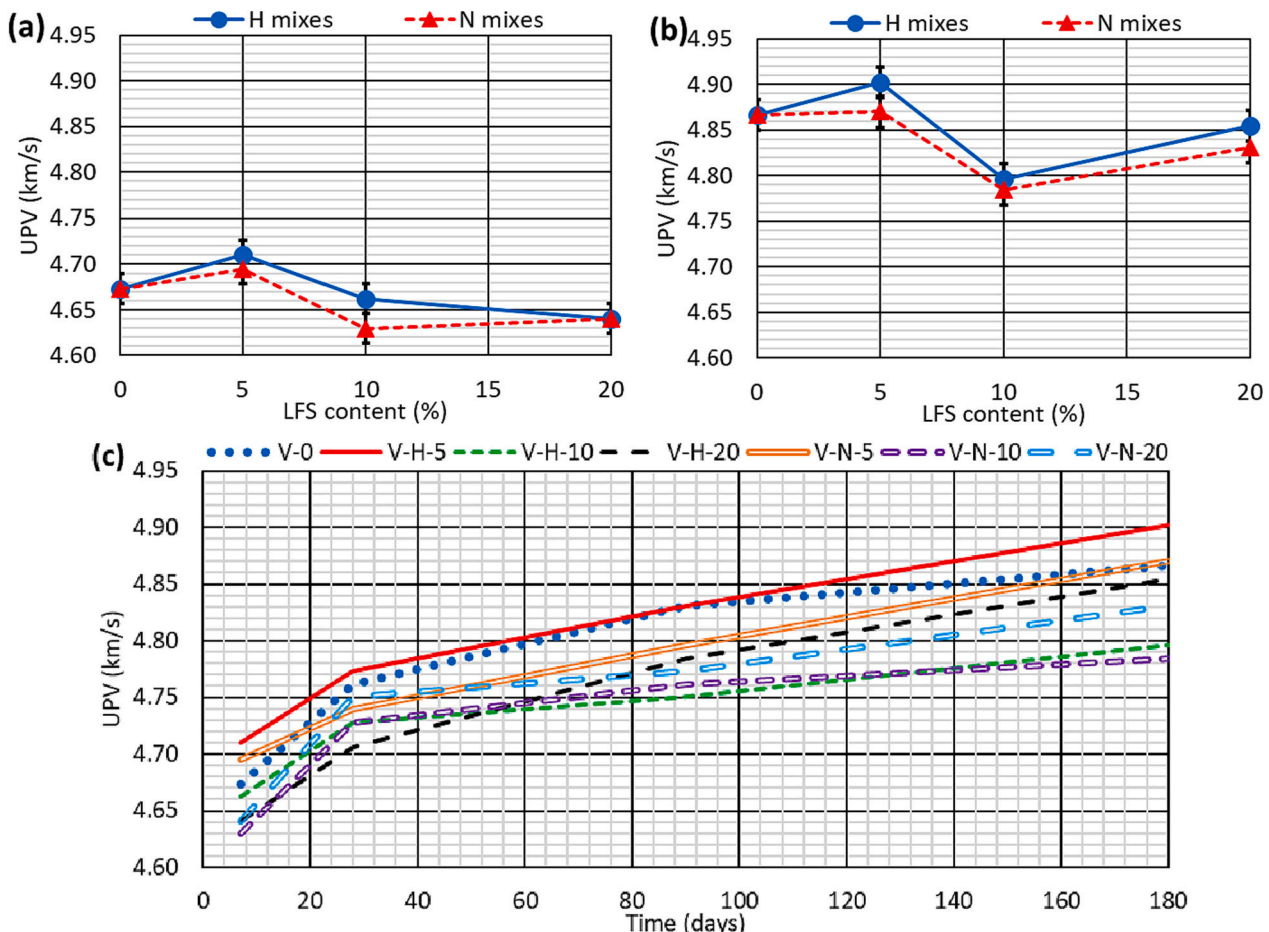


Fig. 9. Ultrasonic pulse velocity: (a) 7-day results; (b) 180-day results; (c) development over time.

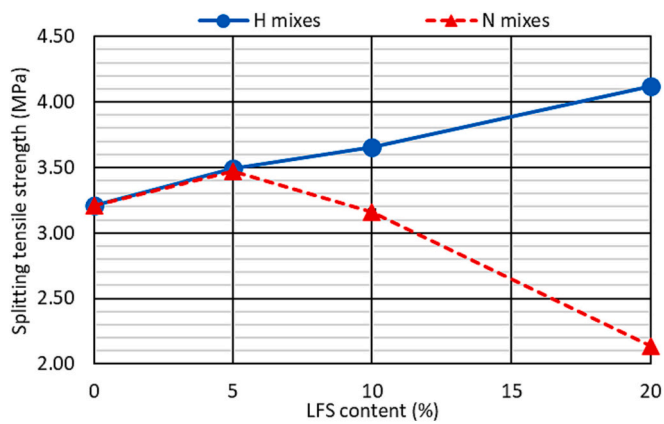


Fig. 10. 28-day splitting tensile strength.

behavior obtained in relation to the increase in the LFS content was largely similar to that of the modulus of elasticity (Fig. 7), the only difference being the effect of the *N*-type LFS for a 10% content.

- Increasing amounts of the *H*-type LFS led to approximately linear increases of splitting tensile strength values. Thus, the splitting tensile strength was 3.21 MPa for the *V-0* control mix and 4.12 MPa for the *V-H-20* mix. As indicated for other mechanical properties, the treatment of this type of LFS prior to its use in the manufacture of concrete could cause it to present low expansiveness [34]. It could mean that the strength-development reactions through C-S-H formation were the most relevant and compensated the negative effect of micro-cracking within the concrete matrix [58], thus increasing the splitting tensile strength.
- Splitting tensile strength is highly dependent on aggregate-and-cementitious-matrix adherence, so it is greatly reduced whenever loading causes aggregate detachment [43,46]. It is thought that the increase in the content of *N*-type LFS and its remarkable expansiveness led to greater micro-cracking concentrated within the interfacial transition zones and favored the detachment of the aggregate, which resulted in a significant decrease in the splitting tensile strength from contents of 10%, so a splitting tensile strength of only 2.14 MPa was obtained for the *V-N-20* mix. This behavior supported the conclusions of the analysis of the modulus of elasticity and related trends, the results of which underlined that the *N*-type LFS could cause micro-cracking concentrated in the interfacial transition zones. Nevertheless, it is important to note that the modulus of elasticity was increased with respect to the control mix when both 5% and 10% of the *N*-type LFS were added. However, the splitting tensile strength increased only minimally in the *V-N-5* mix (3.47 MPa) and then

decreased. It appears that the micro-cracking caused by the *N*-type LFS was more negative under tensile stresses.

Finally, when both types of LFS were compared, the unfavorable effect of micro-cracking associated with the *N*-type LFS could once again be detected. The splitting tensile strength of the *N*-type LFS mixtures was only equal to that of the mixtures with *H*-type LFS for a content of 5%. For the rest of contents, *N*-type LFS provided significantly low splitting tensile strength, reaching a difference of 2 MPa for a content of 20%. Higher moduli of elasticity of the *N*-type LFS mixes with additions of 5% and 10% LFS were observed, which can be explained by the fact that the effect of this type of LFS is more unfavorable under tensile stresses.

3.8. Flexural strength

Flexural strength was also measured at 28 and 90 days, as detailed in Fig. 11, to corroborate the behavior of the mixtures under tensile stresses. Regardless of the LFS content, the evolution of the flexural strength was identical in all the concrete mixes, so LFS never influenced this performance. The behavior found in the flexural strength at both ages was very similar to that of the splitting tensile strength:

- The *H*-type LFS led to an approximately linear increase in flexural strength with the LFS content, so for the *V-H-20* mix a flexural strength between 10% and 25% higher than that of the *V-0* mix was measured. Again, the reduced expansiveness of this type of LFS led to strength-development reactions through the formation of C-S-H gels that increased concrete strength [37,53].
- The *N*-type LFS with additions of 5% led to an increase in flexural strength, with the *V-N-5* mix showing the highest flexural strength at both 28 days (6.59 MPa) and 90 days (7.39 MPa), although flexural strength notably decreased at higher contents. As for the splitting tensile strength, it appeared that the strength development was more remarkable than the expansive micro-cracking for small amounts of the *N*-type LFS [13,31], a performance that was reversed for higher contents.

A comparison between both types of LFS showed that flexural strength depended on both the compressive and the tensile behavior of the concrete specimens [43]. Therefore, the expansiveness of the *N*-type LFS, which had a completely unfavorable effect on the splitting tensile strength, could be compensated here by the formation of C-S-H gel for low LFS contents, so that it provided 0.6–1 MPa higher flexural strengths than the *H*-type LFS for a 5% LFS content. A result quite unlike the splitting tensile strength values, in which 5% additions of the *N*-type LFS only provided equal strengths than the *H*-type LFS and lower strengths for the other amounts. This behavior confirmed that the micro-cracking caused by the *N*-type LFS was more unfavorable under tensile stresses.

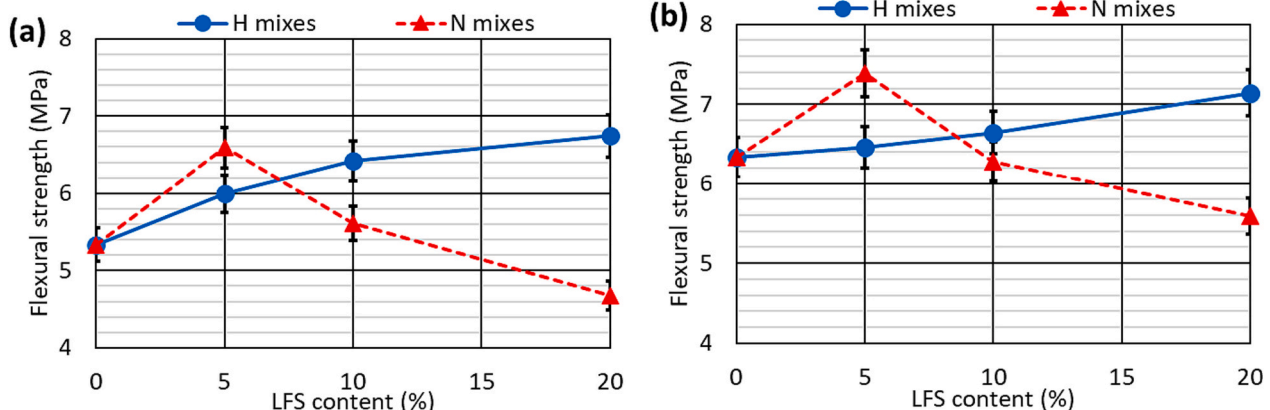


Fig. 11. Flexural strength: (a) 28-day results; (b) 90-day results.

3.9. Micro-structural analysis

As noted in the analysis of the different properties, the micro-cracks that appeared in the cementitious matrix as a consequence of LFS expansion had a significant negative influence on the mechanical behavior of the concrete. Nevertheless, the creation of additional C-S-H gel when adding LFS was beneficial for the mechanical performance of concrete. Fragments of different concrete mixes, extracted from the interior of a cylindrical specimen, were subjected to an SEM analysis, in order to test these hypotheses and to confirm the extent of the micro-cracking and additional C-S-H gel formation. The most representative images are provided in this section.

In Fig. 12, the existence of several micro-cracks can be observed in the interfacial transition zones of the *V-N-20* mix, as well as other cracks within the cementitious matrix that emerged from the pores. These micro-cracks promoted aggregate sliding and a weaker matrix [30]. On the contrary, the hydration of the LFS allowed creating new C-S-H gel and CH plates, as can be observed in the comparison between the *V-0* and *V-H-20* mixes in Fig. 13. Furthermore, almost no voids appeared between the compounds formed because of LFS hydration. Joining both dimensions, when micro-cracks appeared and could not be compensated by the formation of C-S-H gel due to the hydration process of LFS, they led to a worsening of the mechanical properties of concrete, but in some case the new C-S-H improved the mechanical performance.

3.10. Two-way ANalysis of VAriance (ANOVA)

A two-way ANOVA was performed at a 95% confidence level, in order to evaluate whether the variations of the fresh and mechanical properties caused by the addition of different contents and types of LFS (two factors) were significant. Through the ANOVA, homogeneous groups were also determined for each factor, i.e., factor values for which the mechanical properties were statistically equal. All the ANOVA results are shown in Table 5.

The ANOVA showed that the variations in slump, density, and UPV readings caused by LFS addition were not significant. Thus, the same properties were observed in the concrete regardless of the amount and the type of LFS that was incorporated. The LFS had significant effects on all the other properties of the concrete:

- Air content was the fresh property most influenced by LFS additions. Thus, each amount and type of LFS led to a statistically different result. The only situation in which there was no noticeable difference was with additions of either 5% or 10% of the same type of LFS.
- In relation to the compressive-behavior-related properties, it was noted that the performance provided by both LFS types was statistically similar up to 28 days, at which point both types of LFS no longer constituted a homogeneous group. As explained in the literature, LFS undergoes expansion and strength-development reactions mainly in the long term [18,26], which means that both types of LFS produce statistically different results. The LFS content was less relevant, although in general the addition of 20% LFS produced a concrete that was comparable to the control mix, while the difference caused by either 5% or 10% LFS was minimal.
- The effect of LFS on Poisson's coefficient was similar to its effects on compressive strength and the modulus of elasticity. Hence, neither the LFS content nor type affected the value obtained at both 28 and 90 days, while at 180 days the type of LFS did have an influence. The higher expansivity of the *N*-type LFS at advanced ages increased Poisson's coefficient [30], unlike the *H*-type LFS, whose remarkable development of elastic stiffness caused a decrease in the same coefficient.
- Finally, the ANOVA also showed that the effect of each LFS content and type on splitting tensile strength and flexural strength was, in general, completely different. As discussed throughout the study, the *H*-type LFS increased both properties as a consequence of the hydration reactions that produced C-S-H gel [6], whereas micro-cracking caused by expansion was the predominant phenomenon when the *N*-type LFS was added [51]. Thus, the tensile-behavior-related mechanical properties were the most significantly affected by the addition of LFS.

4. Results and discussion: Carbon footprint

Steel slags can be used as a raw material for the production of cement-based materials of very different nature [60,61], one of its main advantages being the increase in sustainability they provide [60–62]. To address this aspect, the carbon footprint of each mix of the study was determined. This calculation was made for comparative purposes, based on the composition of the mixes (Table 3) and the carbon footprint of

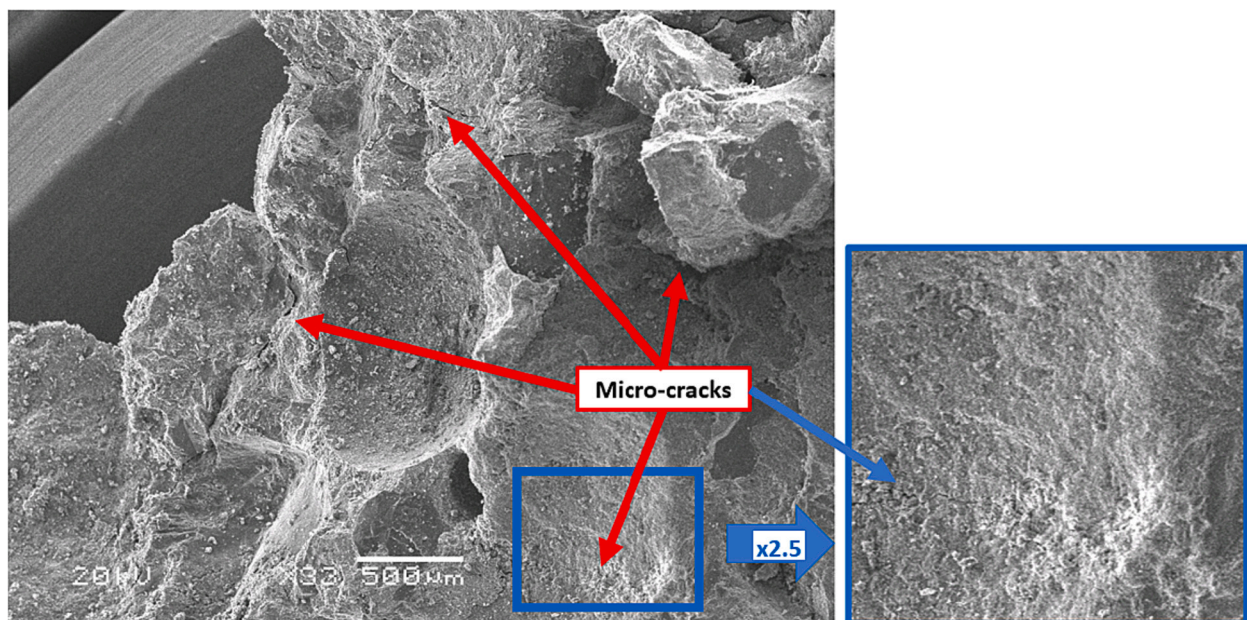


Fig. 12. SEM image of the *V-N-20* mix.

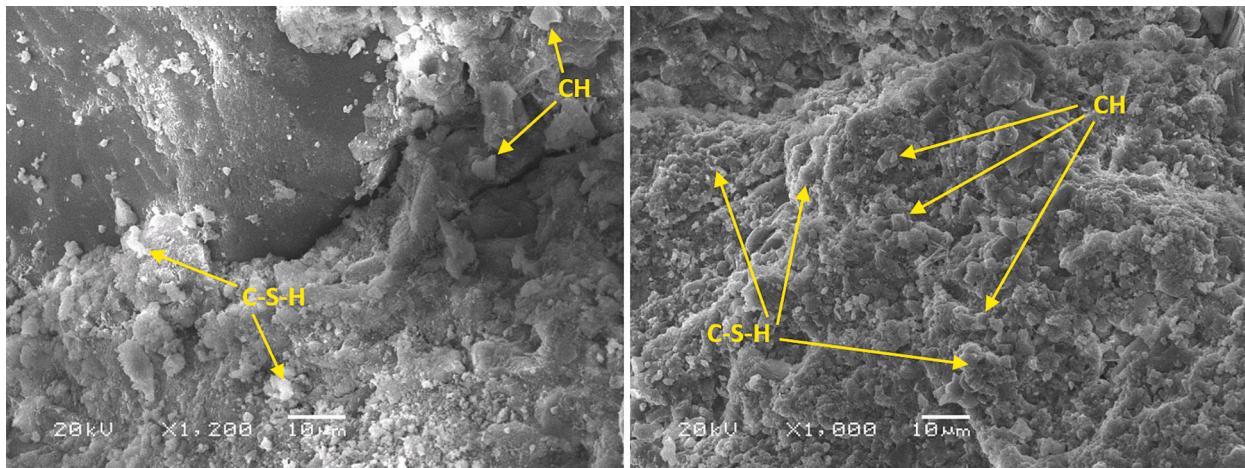


Fig. 13. SEM images of the mixes V-0 (left) and V-H-20 (right).

each one of its raw materials, sourced from other research [63,64]. The results, depicted in Fig. 14, show that both types of LFS effectively reduced the carbon footprint of concrete. The extent of the reduction was more pronounced with higher added contents of this by-product. Specifically, *N*-type LFS exhibited a slightly superior effectiveness in improving the environmental performance of concrete.

5. Results and discussion: Selection of the optimum mix

A multi-criteria decision-making analysis was conducted using two common algorithms for the optimum selection of concrete, TOPSIS and PROMETHEE, and the average ranking was subsequently calculated, in order to determine the optimum type and content of LFS to be used in the production of concrete from the point of view of its mechanical and environmental behavior [65,66]. This analysis considered all the properties evaluated throughout this article, all of them with the same importance. The preference ranking obtained for the different mixes, in Fig. 15, shows the best performing mix as the first and the worst overall performance as the last one.

The multi-criteria analysis showed that the *V-N-5* mix, made with 5% *N*-type LFS, had the best overall performance, immediately followed by the *V-H-20* mix (20% *H*-type LFS); both showing a better overall mechanical performance than the *V-0* control mix. Nevertheless, it can also be perceived that the *H*-type LFS mixtures occupied 2nd, 3rd, and 5th places in the preference ranking (*V-H-20*, *V-H-5* and *V-H-10* mixes, respectively), while the *V-N-10* and *V-N-20* mixes occupied the last two places.

These results clearly recommend the *H*-type LFS for concrete production, as its use guarantees a similar or even better mechanical behavior to concrete produced without this industrial by-product. This recommendation is based on the capacity of this LFS type to provide adequate strength to the concrete without undergoing significant expansion. Therefore, the mechanical and environmental performance of concrete can be successfully improved when the LFS has undergone a prior stabilization process.

6. Conclusions

In this study, the mechanical properties of concrete made with Ladle Furnace Slag (LFS) of two different origins has been evaluated: *H*-type LFS, which was previously subjected to a stabilization process at a steelmaking-waste-management company prior to its landfilling, and *N*-type LFS, which was supplied directly from a ladle furnace, and was therefore in a more unaltered state. In addition, the composition of *N*-type LFS revealed that it had a higher risk of expansion. Contents of 5%, 10%, and 20% in concrete mixes were considered for both LFS types.

The following conclusions can be drawn from the tests that have been performed:

- The concrete slump and fresh density were not affected when adding LFS, regardless of amount and type, thanks to the increase in water content, which compensated for the irregular shape and water consumption, due to chemical reactions. However, air content did increase with the addition of LFS, especially with *N*-type LFS, due to its more irregular shape and higher hydraulic activity.
- The *H*-type LFS had a minimal effect on compressive strength, as the mixes that incorporated it showed a similar compressive strength to the control mix (0% LFS), regardless of the LFS content and concrete age. However, the *N*-type LFS caused an increase in compressive strength with contents up to 10% and a large decrease for higher contents. Thus, it seems that the micro-cracking caused by expansive phenomena was adequately compensated through the formation of Calcium-Silicate-Hydrates (C-S-H) for all the *H*-type LFS contents, whereas both phenomena were more extreme when adding the *N*-type LFS, one or the other predominating, depending on the LFS content. Regardless of the type of LFS, its addition caused more delayed strength development over time.
- The modulus of elasticity was also noticeably modified by adding LFS. Therefore, the increase in the content of *H*-type LFS led to an increase in the modulus of elasticity, due to the development of elastic stiffness by forming C-S-H. Furthermore, the *N*-type LFS increased the modulus of elasticity for 5% and 10% contents, but decreased it markedly with the addition of 20%, in a similar way to the behavior of compressive strength. The LFS expansion and related concrete micro-cracking accentuated transversal deformability to the load direction and, therefore, the Poisson's coefficient. This increase was higher for the *N*-type LFS, while the Poisson's coefficients of the *H*-type LFS mixes decreased at advanced ages, due to their higher elastic-stiffness development.
- The variations of the ultrasonic pulse velocity with the addition of any type of LFS were minimal. The UPV was not affected by the micro-cracking or strength development that this steelmaking slag by-product can cause. Thus, this non-destructive measurement is not suitable for estimating the compressive-behavior-related mechanical properties of LFS mixes.
- The effect of the addition of each type of LFS was shown most clearly in the tensile-behavior-related properties. Increasing the amount of the *H*-type LFS caused a continuous increase in splitting tensile strength and flexural strength, due to the formation of C-S-H gels. However, the micro-cracking due to additions of the *N*-type LFS provoked a decrease in both properties for all contents except for additions of 5%, with which a behavior similar to that obtained with

Table 5
Two-way ANOVA (95% confidence level).

Property	p-values of the factors			Homogeneous groups	
	LFS content	LFS type	Interaction	LFS content	LFS type
Slump	0.2245	0.2637	0.7826	0%, 5%, 10%, and 20%	H and N
Fresh density	0.9973	0.9610	1.0000	0%, 5%, 10%, and 20%	H and N
Air content	0.0001	0.0005	0.0260	5% and 10%	–
28-day hardened density	0.9510	0.7723	0.9947	0%, 5%, 10%, and 20%	H and N
7-day compressive strength	0.0007	0.8844	0.0032	0% and 20%; 5% and 10%	H and N
28-day compressive strength	0.0004	0.0315	0.0005	0% and 20%; 5% and 10%	H and N
90-day compressive strength	0.4188	0.0079	0.0005	0%, 5%, 10%, and 20%	–
180-day compressive strength	0.0129	0.0067	0.0499	0% and 20%; 0%, 5%, and 10%	–
28-day modulus of elasticity	0.0313	0.3388	0.0089	5% and 10%; 10% and 20%; 0% and 20%	H and N
90-day modulus of elasticity	0.0249	0.1997	0.0032	0% and 20%; 0%, 5%, and 10%	–
180-day modulus of elasticity	0.1429	0.0290	0.0007	0%, 5%, 10%, and 20%	–
28-day Poisson's coefficient	0.3095	0.4321	0.5815	0%, 5%, 10%, and 20%	H and N
90-day Poisson's coefficient	0.1369	0.7527	0.6402	0%, 5%, 10%, and 20%	H and N
180-day Poisson's coefficient	0.1429	0.0290	0.0007	0%, 5%, 10%, and 20%	–
7-day UPV	0.9187	0.8707	0.9981	0%, 5%, 10%, and 20%	H and N
28-day UPV	0.9770	0.9705	0.9832	0%, 5%, 10%, and 20%	H and N
90-day UPV	0.8756	0.9049	0.9960	0%, 5%, 10%, and 20%	H and N
180-day UPV	0.7970	0.8190	0.9986	0%, 5%, 10%, and 20%	H and N
28-day splitting tensile strength	0.0252	0.0000	0.0000	–	–
28-day flexural strength	0.0001	0.0000	0.0000	–	–
90-day flexural strength	0.0012	0.0080	0.0000	0% and 10%	–

5% H-type LFS was achieved. Micro-cracking in the concrete matrix might perhaps be associated with the N-type LFS that favored aggregate detachment. These aspects were verified through Scanning Electron Microscopy.

Through a global perspective, it can be concluded that the H-type LFS, which underwent a stabilization treatment prior to its use, improved the mechanical properties and carbon footprint of the concrete. Therefore, this type of LFS is preferable in the production of concrete with respect to non-pretreated LFS (N-type LFS), as is also

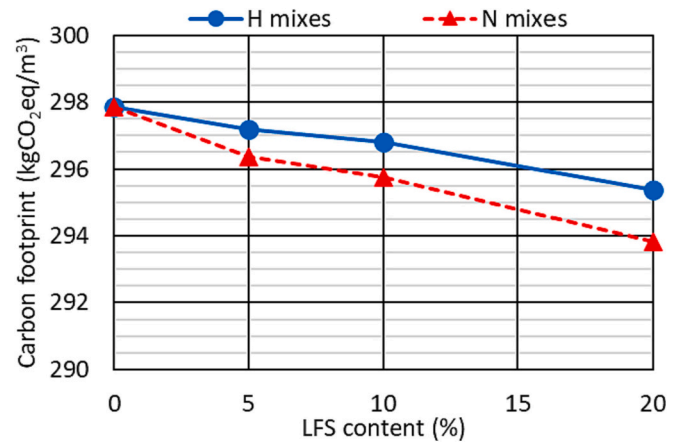


Fig. 14. Carbon footprint of the concrete mixes.

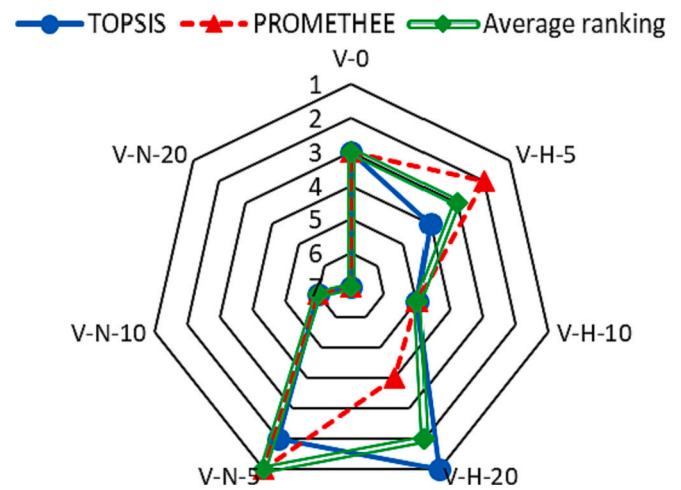


Fig. 15. Preference order for concrete mix selection.

reflected by a multi-criteria decision-making analysis. However, it should also be noted that the difference in the mechanical properties of the concretes produced with both types of LFS was only significant at advanced ages as per the analysis of variance conducted.

CRedit authorship contribution statement

Víctor López-Ausín: Writing – review & editing, Visualization, Validation, Software, Methodology, Formal analysis. **Víctor Revilla-Cuesta:** Writing – original draft, Validation, Methodology, Investigation, Formal analysis, Conceptualization. **Marta Skaf:** Writing – review & editing, Supervision, Methodology, Investigation, Funding acquisition, Data curation, Conceptualization. **Vanesa Ortega-López:** Writing – review & editing, Supervision, Resources, Project administration, Data curation, Conceptualization.

Declaration of competing interest

The authors declare that they have no known competing financial interests or personal relationships that could have appeared to influence the work reported in this paper.

Data availability

Data will be made available on request.

Acknowledgements

This research work was supported by the Spanish Ministry of Universities, MICINN, AEI, EU, ERDF and NextGenerationEU/PRTR [grant numbers PID2020-113837RB-I00; 10.13039/501100011033; TED2021-129715B-I00]; the Junta de Castilla y León (Regional Government) and ERDF [grant number UIC-231; BU033P23]; and, finally, the University of Burgos [grant number SUCONS, Y135.GI].

References

- F. de Andrade Salgado, F. de Andrade Silva, Recycled aggregates from construction and demolition waste towards an application on structural concrete: a review, *J. Build. Eng.* 52 (2022) 104452, <https://doi.org/10.1016/j.jobe.2022.104452>.
- R. Rodríguez-Alvaro, S. Seara-Paz, B. González-Fontebo, M. Etxeberria, Study of different granular by-products as internal curing water reservoirs in concrete, *J. Build. Eng.* 45 (2022) 103623, <https://doi.org/10.1016/j.jobe.2021.103623>.
- K. Nandhini, J. Karthikeyan, A review on sustainable production of self-compacting concrete utilizing industrial by-products as cementitious materials, *Innov. Infrastruct. Solut.* 7 (3) (2022) 199, <https://doi.org/10.1007/s41062-022-00792-1>.
- M.A. Peñaranda Barba, V. Alarcón Martínez, I. Gómez Lucas, J. Navarro Pedreño, Mitigation of environmental impacts in ornamental rock and limestone aggregate quarries in arid and semi-arid areas, *Glob. J. Environ. Sci. Manag.* 7 (4) (2021) 565–586.
- R. Osiris de León, Environmental problematic about of fluviatile aggregates extraction process in the Dominican Republic and the alternative solutions, *Bol. Geol. Min.* 117 (4) (2006) 747–762.
- Z.H. He, X.D. Han, M.Y. Zhang, Q. Yuan, J.Y. Shi, P.M. Zhan, A novel development of green UHPC containing waste concrete powder derived from construction and demolition waste, *Powder Technol.* 398 (2022) 117075, <https://doi.org/10.1016/j.powtec.2021.117075>.
- M. Amran, N. Makul, R. Fediuk, Y.H. Lee, N.I. Vatin, Y.Y. Lee, K. Mohammed, Global carbon recoverability experiences from the cement industry, *Case Stud. Constr. Mater.* 17 (2022) e01439, <https://doi.org/10.1016/j.cscm.2022.e01439>.
- G. Xu, D. Xue, H. Rehman, Dynamic scenario analysis of CO₂ emission in China's cement industry by 2100 under the context of cutting overcapacity, *Mitig. Adapt. Strateg. Glob. Chang.* 27 (8) (2022) 53, <https://doi.org/10.1007/s11027-022-10028-3>.
- World Steel Association, *Steel Statistical Yearbook*, World Steel Association, Brussels, Belgium, 2022.
- M. Sambandam, V.N. Nurni, S.P. Jayaraj, Sustainable production of steel-carbon neutrality and low life cycle emission, *J. Indian Inst. Sci.* 102 (1) (2022) 117–126, <https://doi.org/10.1007/s41745-021-00285-7>.
- I.H. Aziz, M.M.A.B. Abdullah, M.A.A.M. Salleh, L.Y. Ming, L.Y. Li, A.V. Sandu, P. Vizureanu, O. Nemes, S.N. Mahdi, Recent developments in steelmaking industry and potential alkali activated based steel waste: a comprehensive review, *Materials* 15 (5) (2022) 1948, <https://doi.org/10.3390/ma15051948>.
- U.S. Geological Survey, *Iron and steel slag*, U.S. Geological Survey, Mineral Commodity Summaries, Reston, VA, 2022.
- I.Z. Yildirim, M. Prezzi, Chemical, mineralogical, and morphological properties of steel slag, *Adv. Civ. Eng.* 2011 (2011) 463638, <https://doi.org/10.1155/2011/463638>.
- A.M. Rashad, Behavior of steel slag aggregate in mortar and concrete - a comprehensive overview, *J. Build. Eng.* 53 (2022) 104536, <https://doi.org/10.1016/j.jobe.2022.104536>.
- A. Santamaría, V. Ortega-López, M. Skaf, J.A. Chica, J.M. Manso, The study of properties and behavior of self compacting concrete containing electric arc furnace slag (EAFS) as aggregate, *Ain. Shams Eng. J.* 11 (1) (2020) 231–243, <https://doi.org/10.1016/j.asej.2019.10.001>.
- I. Arribas, J. San-José, I. Vegas, J. Hurtado, J. Chica, Application of steel slag concrete in the foundation slab and basement wall of the Tecnalia kubik building, in: *6th European Slag Conference Proceedings, Madrid, Euroslag, 2010*, pp. 251–264.
- X. Lyu, N. Robinson, M. Elchalakani, M.L. Johns, M. Dong, S. Nie, Sea sand seawater geopolymer concrete, *J. Build. Eng.* 50 (2022) 104141, <https://doi.org/10.1016/j.jobe.2022.104141>.
- O. Gencel, O. Karadag, O.H. Oren, T. Bilir, Steel slag and its applications in cement and concrete technology: a review, *Constr. Build. Mater.* 283 (2021) 122783, <https://doi.org/10.1016/j.conbuildmat.2021.122783>.
- V. Ortega-López, M. Skaf, A. Santamaría, The reuse of ladle furnace basic slags in clayey soil-stabilization applications, *soil Stabil.: types, Methods Appl.* (2017) 231–271.
- R. Ashwathi, G.T. Amudhan Vetrivel, M. Abishek, Investigation on strength properties of concrete using steel slag as a partial replacement for fine aggregate, *Mater. Res. Proc.* 23 (2022) 401–418, <https://doi.org/10.21741/9781644901953-44>.
- M.H. Lai, J. Zou, B. Yao, J.C.M. Ho, X. Zhuang, Q. Wang, Improving mechanical behavior and microstructure of concrete by using BOF steel slag aggregate, *Constr. Build. Mater.* 277 (2021) 122269, <https://doi.org/10.1016/j.conbuildmat.2021.122269>.
- E. Özbay, M. Erdemir, H.I. Durmuş, Utilization and efficiency of ground granulated blast furnace slag on concrete properties - a review, *Constr. Build. Mater.* 105 (2016) 423–434, <https://doi.org/10.1016/j.conbuildmat.2015.12.153>.
- A.L. Beaucour, P. Pliya, F. Faleschini, R. Njinwoua, C. Pellegrino, A. Noumowé, Influence of elevated temperature on properties of radiation shielding concrete with electric arc furnace slag as coarse aggregate, *Constr. Build. Mater.* 256 (2020) 119385, <https://doi.org/10.1016/j.conbuildmat.2020.119385>.
- A. Santamaría, A. Orbe, M.M. Losañez, M. Skaf, V. Ortega-López, J.J. González, Self-compacting concrete incorporating electric arc-furnace steelmaking slag as aggregate, *Mater. Des.* 115 (2017) 179–193, <https://doi.org/10.1016/j.matdes.2016.11.048>.
- V. Ortega-López, V. Revilla-Cuesta, A. Santamaría, A. Orbe, M. Skaf, Microstructure and dimensional stability of slag-based high-workability concrete with steelmaking slag aggregate and fibers, *J. Mater. Civ. Eng.* 34 (9) (2022) 04022224, [https://doi.org/10.1061/\(ASCE\)MT.1943-5533.0004372](https://doi.org/10.1061/(ASCE)MT.1943-5533.0004372).
- A. Santamaría, J.J. González, M.M. Losañez, M. Skaf, V. Ortega-López, The design of self-compacting structural mortar containing steelmaking slags as aggregate, *Cem. Concr. Compos.* 111 (2020) 103627, <https://doi.org/10.1016/j.cemconcomp.2020.103627>.
- M. Mahoutian, Y. Shao, Low temperature synthesis of cement from ladle slag and fly ash, *J. Sustain. Cem. Based Mater.* 5 (4) (2016) 247–258, <https://doi.org/10.1080/21650373.2015.1047913>.
- Y. Jiang, T.C. Ling, C. Shi, S.Y. Pan, Characteristics of steel slags and their use in cement and concrete—a review, *Resour. Conserv. Recycl.* 136 (2018) 187–197, <https://doi.org/10.1016/j.resconrec.2018.04.023>.
- A.C.P. Martins, J.M. Franco de Carvalho, L.C.B. Costa, H.D. Andrade, T.V. de Melo, J.C.L. Ribeiro, L.G. Pedroti, R.A.F. Peixoto, Steel slags in cement-based composites: an ultimate review on characterization, applications and performance, *Constr. Build. Mater.* 291 (2021) 123265, <https://doi.org/10.1016/j.conbuildmat.2021.123265>.
- A. Rodríguez, I. Santamaría-Vicario, V. Calderón, C. Junco, J. García-Cuadrado, Study of the expansion of cement mortars manufactured with ladle furnace slag LFS, *Mater. Constr.* 69 (334) (2019) e183, <https://doi.org/10.3989/mc.2019.06018>.
- V. Ortega-López, J.M. Manso, I.I. Cuesta, J.J. González, The long-term accelerated expansion of various ladle-furnace basic slags and their soil-stabilization applications, *Constr. Build. Mater.* 68 (2014) 455–464, <https://doi.org/10.1016/j.conbuildmat.2014.07.023>.
- M. Skaf, V. Ortega-López, V. Revilla-Cuesta, J.M. Manso, Bituminous pavement overlay of a porous asphalt mixture with ladle furnace slag: a pilot project, *Road Mater. Pavement Des.* 24 (2) (2023) 2780–2793, <https://doi.org/10.1080/14680629.2022.2154251>.
- V. Pachta, E.K. Anastasiou, Utilization of industrial byproducts for enhancing the properties of cement mortars at elevated temperatures, *Sustainability* 13 (21) (2021) 12104, <https://doi.org/10.3390/su132112104>.
- P. Araos Henríquez, D. Aponte, J. Ibáñez-Insa, M. Barra Bizinotto, Ladle furnace slag as a partial replacement of Portland cement, *Constr. Build. Mater.* 289 (2021) 123106, <https://doi.org/10.1016/j.conbuildmat.2021.123106>.
- V. Ortega-López, A. García-Llona, V. Revilla-Cuesta, A. Santamaría, J.T. San-José, Fiber-reinforcement and its effects on the mechanical properties of high-workability concretes manufactured with slag as aggregate and binder, *J. Build. Eng.* 43 (2021) 102548, <https://doi.org/10.1016/j.jobe.2021.102548>.
- A.S. Brand, E.O. Fanijo, A review of the influence of steel furnace slag type on the properties of cementitious composites, *Appl. Sci.* 10 (22) (2020) 8210, <https://doi.org/10.3390/app10228210>.
- K.K. Sideris, C. Tassos, A. Chatzopoulos, P. Manita, Mechanical characteristics and durability of self compacting concretes produced with ladle furnace slag, *Constr. Build. Mater.* 170 (2018) 660–667, <https://doi.org/10.1016/j.conbuildmat.2018.03.091>.
- J.A. Polanco, J.M. Manso, J. Setién, J.J. González, Strength and durability of concrete made with electric steelmaking slag, *ACI Mater. J.* 108 (2) (2011) 196–203.
- V. López-Ausín, V. Revilla-Cuesta, M. Skaf, A.B. Espinosa, J.M. Manso, Modification of shrinkage and mechanical properties of concrete by the addition of ladle furnace slag (LFS), *Mater. Today Proc.* (2023), <https://doi.org/10.1016/j.matpr.2023.03.689>.
- V. Revilla-Cuesta, R. Serrano-López, A.B. Espinosa, V. Ortega-López, M. Skaf, Analyzing the relationship between compressive strength and Modulus of elasticity in concrete with ladle furnace slag, *Buildings* 13 (12) (2023) 3100, <https://doi.org/10.3390/buildings13123100>.
- EN-Euronorm, *Rue de stassart, 36. Belgium-1050 Brussels, European Committee for Standardization*.
- D. Zhang, B. Jaworska, H. Zhu, K. Dahlquist, V.C. Li, Engineered cementitious composites (ECC) with limestone calcined clay cement (LC3), *Cem. Concr. Compos.* 114 (2020) 103766, <https://doi.org/10.1016/j.cemconcomp.2020.103766>.
- V. Revilla-Cuesta, F. Faleschini, M.A. Zanini, M. Skaf, V. Ortega-López, Porosity-based models for estimating the mechanical properties of self-compacting concrete with coarse and fine recycled concrete aggregate, *J. Build. Eng.* 44 (2021) 103425, <https://doi.org/10.1016/j.jobe.2021.103425>.
- EC-2, *Eurocode 2: Design of Concrete Structures. Part 1–1: General Rules and Rules for Buildings*, CEN (European Committee for Standardization), 2010.
- Structural Code, *Código Estructural de España. Spanish Structural Code*, Ministerio de Fomento, Gobierno de España, 2021.
- M. Bravo, J. De Brito, J. Pontes, L. Evangelista, Mechanical performance of concrete made with aggregates from construction and demolition waste recycling plants, *J. Clean. Prod.* 99 (2015) 59–74, <https://doi.org/10.1016/j.jclepro.2015.03.012>.
- D. Zawal, A.M. Grabiec, Influence of selected mineral additives on properties of recycled aggregate concrete (RAC) considering eco-efficiency coefficients, *Case*

- Stud. Constr. Mater. 17 (2022) e01405, <https://doi.org/10.1016/j.cscm.2022.e01405>.
- [48] R.V. Silva, J. de Brito, R.K. Dhir, Fresh-state performance of recycled aggregate concrete: a review, *Constr. Build. Mater.* 178 (2018) 19–31, <https://doi.org/10.1016/j.conbuildmat.2018.05.149>.
- [49] A. Santamaría, V. Ortega-López, M. Skaf, F. Faleschini, A. Orbe, J.T. San-José, Ladle furnace slags for construction and civil works: a promising reality, *Waste Byproducts Cement-Based Mater.* (2021) 659–679, <https://doi.org/10.1016/B978-0-12-820549-5.00023-1>.
- [50] T. Gonçalves, R.V. Silva, J. de Brito, J.M. Fernández, A.R. Esquinas, Mechanical and durability performance of mortars with fine recycled concrete aggregates and reactive magnesium oxide as partial cement replacement, *Cem. Concr. Compos.* 105 (2020) 103420, <https://doi.org/10.1016/j.cemconcomp.2019.103420>.
- [51] V. Revilla-Cuesta, L. Evangelista, J. de Brito, M. Skaf, V. Ortega-López, Mechanical performance and autogenous and drying shrinkage of MgO-based recycled aggregate high-performance concrete, *Constr. Build. Mater.* 314 (2022) 125726, <https://doi.org/10.1016/j.conbuildmat.2021.125726>.
- [52] N. José, H. Ahmed, B. Miguel, E. Luís, B. Jorge, Magnesia (Mgo) production and characterization, and its influence on the performance of cementitious materials: a review, *Materials* 13 (21) (2020) 4752, <https://doi.org/10.3390/ma13214752>.
- [53] J.M. Manso, M. Losañez, J.A. Polanco, J.J. Gonzalez, Ladle furnace slag in construction, *J. Mater. Civ. Eng.* 17 (5) (2005) 513–518, [https://doi.org/10.1061/\(ASCE\)0899-1561\(2005\)17:5\(513\)](https://doi.org/10.1061/(ASCE)0899-1561(2005)17:5(513)).
- [54] V. Revilla-Cuesta, M. Skaf, A. Santamaría, J.M. Romera, V. Ortega-López, Elastic stiffness estimation of aggregate-ITZ system of concrete through matrix porosity and volumetric considerations: explanation and exemplification, *Arch. Civ. Mech. Eng.* 22 (2) (2022) 59, <https://doi.org/10.1007/s43452-022-00382-z>.
- [55] C. Shi, S. Hu, Cementitious properties of ladle slag fines under autoclave curing conditions, *Cem. Concr. Res.* 33 (11) (2003) 1851–1856, [https://doi.org/10.1016/S0008-8846\(03\)00211-4](https://doi.org/10.1016/S0008-8846(03)00211-4).
- [56] I.R. Mocharla, R. Selvam, V. Govindaraj, M. Muthu, Performance and life-cycle assessment of high-volume fly ash concrete mixes containing steel slag sand, *Constr. Build. Mater.* 341 (2022) 127814, <https://doi.org/10.1016/j.conbuildmat.2022.127814>.
- [57] V.M. Malhotra, *Testing Hardened Concrete: Nondestructive Methods*, American Concrete Institute Monograph no. 9, Iowa State University Press, Ames IA, USA, 1976.
- [58] N. Singh, S.P. Singh, Evaluating the performance of self compacting concretes made with recycled coarse and fine aggregates using non destructive testing techniques, *Constr. Build. Mater.* 181 (2018) 73–84, <https://doi.org/10.1016/j.conbuildmat.2018.06.039>.
- [59] D. Suescum-Morales, R.V. Silva, M. Bravo, J.R. Jiménez, J.M. Fernández-Rodríguez, J. de Brito, Effect of incorporating municipal solid waste incinerated bottom ash in alkali-activated fly ash concrete subjected to accelerated CO2 curing, *J. Clean. Prod.* 370 (2022) 133533, <https://doi.org/10.1016/j.jclepro.2022.133533>.
- [60] P. Zhan, J. Xu, J. Wang, J. Zuo, Z. He, Structural supercapacitor electrolytes based on cementitious composites containing recycled steel slag and waste glass powders, *Cem. Concr. Compos.* 137 (2023) 104924, <https://doi.org/10.1016/j.cemconcomp.2022.104924>.
- [61] P.M. Zhan, X.X. Zhang, Z.H. He, J.Y. Shi, O. Gencel, N.T. Hai Yen, G.C. Wang, Strength, microstructure and nanomechanical properties of recycled aggregate concrete containing waste glass powder and steel slag powder, *J. Clean. Prod.* 341 (2022) 130892, <https://doi.org/10.1016/j.jclepro.2022.130892>.
- [62] J. Xu, P. Zhan, W. Zhou, J. Zuo, S.P. Shah, Z. He, Design and assessment of eco-friendly ultra-high performance concrete with steel slag powder and recycled glass powder, *Powder Technol.* 419 (2023) 118356, <https://doi.org/10.1016/j.powtec.2023.118356>.
- [63] M.U. Hossain, C.S. Poon, I.M.C. Lo, J.C.P. Cheng, Comparative environmental evaluation of aggregate production from recycled waste materials and virgin sources by LCA, *Resour. Conserv. Recycl.* 109 (2016) 67–77, <https://doi.org/10.1016/j.resconrec.2016.02.009>.
- [64] K.H. Yang, Y.B. Jung, M.S. Cho, S.H. Tae, Effect of supplementary cementitious materials on reduction of CO2 emissions from concrete, *J. Clean. Prod.* 103 (2015) 774–783, <https://doi.org/10.1016/j.jclepro.2014.03.018>.
- [65] M. Abed, K. Rashid, M.U. Rehman, M. Ju, Performance keys on self-compacting concrete using recycled aggregate with fly ash by multi-criteria analysis, *J. Clean. Prod.* 378 (2022) 134398, <https://doi.org/10.1016/j.jclepro.2022.134398>.
- [66] D. Merachtsaki, S. Tsiaras, E. Peleka, A. Zouboulis, Selection of magnesium hydroxide coatings for corrosion mitigation in concrete sewer pipes by using multiple criteria decision analysis, *Environ. Sustain. Ind.* 13 (2022) 100168, <https://doi.org/10.1016/j.indic.2021.100168>.